SAND2010-1057C

Uses and Efficient Evaluation of Half-Line Source Potentials and Their Derivatives

F. T. Celepcikay[1 #], D. R. Wilton[1], D. R. Jackson[1], S. Paulotto[1], and W. A. Johnson[2]

[1]*Department of Electrical and Computer Engineering*
University of Houston, Houston, TX 77204-4005, USA

[2]*Electromagnetic Effects Department*
Sandia National Laboratories
Albuquerque, NM 87185, USA

[#] ferhat.celepcikay@mail.uh.edu

***Abstract*— In this paper three different methods are examined to evaluate the potential due to a half-line source. They are compared in terms of accuracy and computational cost in order to find the best scheme for each region of space.**

I. Introduction

Recently, a wide spectrum of applications has emerged that utilize one- or two-dimensional periodic structures in layered media. For this reason, the fast and accurate evaluation of periodic Green's functions in layered-media has received increasing attention. Both Ewald transformations and interpolation techniques have been used to accelerate the computation of these Green's functions. The usual acceleration techniques identify and remove asymptotic terms in the spectral sums that correspond to a periodic array of point sources in an infinite homogeneous medium. This type of extraction not only accelerates the convergence of the spectral sum, but also creates a "regularized" Green's function that is much smoother as a function of spatial coordinates, and hence is much easier to interpolate.

The extraction of terms corresponding to a periodic array of point sources is all that is needed when analysing planar sources in layered media. However, the situation is more complicated when treating arbitrarily-oriented sources within layered media. In particular, the components of the dyadic and scalar layered-media Green's functions that arise from vertical currents have a faster asymptotic rate of decay in their spectral sums. Indeed, it may be shown that the asymptotic extractions from the spectral sums correspond in the spatial domain to an infinite periodic array of half-line sources. The computation of the potential produced by a periodic array of half-line sources in a homogeneous medium thus becomes an important problem. This potential may be regularized within a unit cell by removing the contributions from the individual (non-periodic) half line sources located at the corners of the unit cell. Hence, the efficient evaluation of the scalar Green's function due to a single half-line source is a key element in the efficient calculation of the periodic layered-media Green's function.

In this paper, we examine three different methods to evaluate the potential due to a half-line source. This potential depends only on two variables, $k\rho$ and kz, where $k = 2\pi/\lambda$, i.e., on the electrical distances from the source axis and source tip, respectively, as illustrated in Fig. 1 below. The proposed methods are compared in terms of their computational cost in the (ρ, z) plane.

II. Development Of Methods

The computation of the mixed-potential Green's functions for electric currents involves the dyadic potential Green's function

$$\underline{\mathbf{G}}^A(\mathbf{r},\mathbf{r}') = \begin{bmatrix} G_{xx}^A & 0 & 0 \\ 0 & G_{yy}^A & 0 \\ G_{zx}^A & G_{zy}^A & G_{zz}^A \end{bmatrix}$$

along with the scalar potential Green's functions $K^{\Phi}(\mathbf{r},\mathbf{r}')$ and $P_z(\mathbf{r},\mathbf{r}')$ [1]. The latter leads to the evaluation of the half-line source potential G_z, while the terms G_{zx}^A and G_{zy}^A require its gradient, $\nabla_t G_z$, in the *x-y* plane. Furthermore, the double gradient, $\nabla_t \nabla_t G_z$, is required in the construction of near fields and in the calculation of $\nabla \times \underline{\mathbf{G}}^A$. Hence, it is of interest to calculate not only G_z, but also $\nabla_t G_z$ and $\nabla_t \nabla_t G_z$. In this summary, however, we confine our attention to the calculation of G_z only.

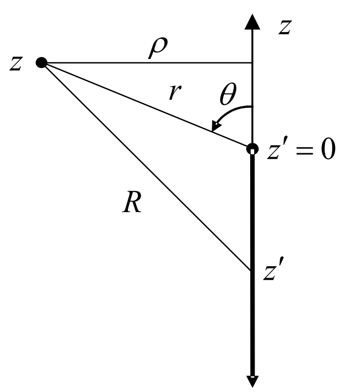

Figure 1. Half-line source with the relevant coordinate system and geometrical parameters defined.

A. Method I: Exponential Integral Representation

Using $z'' = z - z'$, the half-line source potential from the single half-line source shown in Fig. 1 is given by

$$G_z(\rho, z) = \int_z^{\infty} \frac{e^{-jkR}}{4\pi R} dz'', \tag{1}$$

where

$$R \equiv \sqrt{\rho^2 + z''^2} \ .$$

It is assumed here that $z \geq 0$, which corresponds to the practical case encountered in the asymptotic extraction process. (For $z < 0$ the potential may be written as that of an infinite line source minus a contribution that is identical in form to the one shown in (1).) Since $R\,dR = z''\,dz''$, the above can be written as

$$\begin{aligned} \int_z^{\infty} \frac{e^{-jkR}}{4\pi R} dz'' &= \int_r^{\infty} \frac{e^{-jkR}}{4\pi\sqrt{R^2 - \rho^2}} dR \\ &= \int_r^{\infty} \frac{e^{-jkR}}{4\pi R}\left[\sum_{n=0}^{\infty} C_n \left(\frac{\rho}{R}\right)^{2n}\right] dR \ , \end{aligned} \tag{2}$$

where $r = \sqrt{\rho^2 + z^2}$ and the binomial expansion coefficients of the factor

$$\left(R^2 - \rho^2\right)^{-\frac{1}{2}} = R^{-1}\left[1 - \left(\frac{\rho}{R}\right)^2\right]^{-\frac{1}{2}} = R^{-1}\left[\sum_{n=0}^{\infty} C_n \left(\frac{\rho}{R}\right)^{2n}\right] \tag{3}$$

are

$$C_0 = 1, \ C_n = \frac{1 \cdot 3 \cdot 5 \cdots (2n-1)}{2 \cdot 4 \cdot 6 \cdots (2n)} = \frac{(2n-1)}{(2n)} C_{n-1} \ . \tag{4}$$

Interchanging summation and integration and setting $t = R/r$ allows the resulting integrals to be identified as the exponential integrals, defined as

$$E_n(z) \equiv \int_1^{\infty} t^{-n} e^{-zt} dt \ .$$

This yields the result

$$G_z(\rho, z) = \frac{1}{4\pi} \sum_{n=0}^{\infty} C_n \left(\frac{\rho}{r}\right)^{2n} E_{2n+1}(jkr) \ , \tag{5}$$

and the recurrence relation [2]

$$E_{n+1}(z) = \frac{1}{n}\left(e^{-z} - zE_n(z)\right), \ n = 1, 2, 3, \ldots \tag{6}$$

permits all of the exponential integrals to be computed in terms of $E_1(z)$, which minimizes the computational burden of calculating the series (5). This approach is expected to work efficiently for small values of θ (see Fig. 1), corresponding to small values of (ρ/r), where the series (5) converges rapidly. On the other hand, the series in (5) converges slower as the angle θ increases, with the convergence rate becoming too slow to be useful as θ approaches $90°$. This is the motivation for having alternative methods for calculating the half-line source potential, discussed below in Sections B and C.

B. Method II: Numerical Integration

In this approach, we write

$$G_z = \int_z^{\infty} \frac{e^{-jkR}}{4\pi R} dz'' = \int_0^{\infty} \frac{e^{-jkR}}{4\pi R} dz'' - \int_0^{z} \frac{e^{-jkR}}{4\pi R} dz'' \ . \tag{7}$$

The first integral on the right-hand side of (7) is identified as one-half the contribution of an infinite line source, and hence it is known analytically in terms of the Hankel function of the second kind of order zero as

$$\int_0^{\infty} \frac{e^{-jkR}}{4\pi R} dz'' = \frac{1}{8j} H_0^{(2)}(k\rho), \tag{8}$$

whereas the last integral in (7) is treated numerically. This last integral physically corresponds to calculating the potential of a line-source segment extending from $z' = 0$ to $z' = z$. Although a direct numerical evaluation of the last integral in (7) could certainly be performed, the substitution

$$du = \frac{dz''}{R} \ , \tag{9}$$

corresponding to the change of variables

$$u = \sinh^{-1} \frac{z''}{\rho} \ ,$$

removes the near-singular behavior of the integrand, yielding

$$\int_0^{z} \frac{e^{-jkR}}{4\pi R} dz'' = \frac{1}{4\pi} \int_0^{\sinh^{-1}\frac{z}{\rho}} e^{-jkR} du, \tag{10}$$

where

$$R = \rho \cosh u.$$

This integral may be efficiently evaluated using a simple five-point Gauss-Legendre quadrature rule on subintervals representing quarter-cycle variations of the phase term kR.

This approach (method II) is expected to work well for moderate or large (near $90°$) values of θ, where the integrand of (10) varies relatively slowly. For small angles θ, the numerical integration of (10) may suffer from a numerical problem arising from the behavior of the integrand, namely that the $\cosh(u)$ term becomes large before the limit of integration is reached, since the upper limit of integration increases as the angle θ decreases. On the other hand, for small θ, method I becomes very efficient. Thus, method II is not used for small angles θ, as discussed in more detail in the Results section.

C. Method III: Power Series

Although method II works well for moderate and large angles θ, an even more efficient method may be formulated for large angles (angles near 90^o). The last integral in (7) may be written as

$$\frac{1}{4\pi}\int_0^z \frac{e^{-jk\sqrt{z''^2+\rho^2}}}{\sqrt{z''^2+\rho^2}}dz' = \frac{1}{4\pi}\int_0^z \frac{e^{-jk\rho\sqrt{1+(z''/\rho)^2}}}{\rho\sqrt{1+(z''/\rho)^2}}dz'$$
$$= \frac{e^{-jk\rho}}{4\pi}\int_0^{z/\rho} \frac{e^{-jk\rho\left(\sqrt{1+w^2}-1\right)}}{\sqrt{1+w^2}}dw, \qquad (11)$$

where the substitution $w = z''/\rho$ has been made and a leading exponential term has been factored out. Using a Taylor series expansion of the resulting integrand yields the form

$$\frac{e^{-jk\rho\sqrt{1+w^2}}}{\sqrt{1+w^2}} = e^{-jk\rho}\left(1+\sum_{n=1}^{\infty} B_n w^{2n}\right).$$

A term-by-term integration of the series on the right then yields the following series representation of (11):

$$\int_0^z \frac{e^{-jkR}}{4\pi R}dz'' = \frac{e^{-jk\rho}}{4\pi}\frac{z}{\rho}\left(1+\sum_{n=1}^{\infty} B_n\left(\frac{1}{2n+1}\right)\left(\frac{z}{\rho}\right)^{2n}\right). \qquad (12)$$

The first few coefficients of the Taylor series are

$$B_1 = -\frac{1}{2}(1+jk\rho)\ , \quad B_2 = \frac{3}{8}(1+jk\rho)+\frac{(jk\rho)^2}{8}\ ,$$
$$B_3 = -\frac{5}{16}(1+jk\rho)-\frac{1}{8}(jk\rho)^2-\frac{1}{48}(jk\rho)^3,$$
$$B_4 = \frac{35}{128}(1+jk\rho)+\frac{15}{128}(jk\rho)^2+\frac{5}{192}(jk\rho)^3+\frac{1}{384}(jk\rho)^4.$$

This approach (method III) is expected to work efficiently for θ near $90°$, where the series (12) converges rapidly. Thus, the method is complementary to method I.

III. Results

The three proposed methods have been examined and compared in terms of efficiency and accuracy in evaluating the potential of the half-line source. The spatial regions of the (ρ, z) plane for which each method is most efficient for a given accuracy may thus be identified.

Method I (complex exponential integral) and method II (numerical integration) are examined first. Over the (ρ, z) plane, the cost (computation time) associated with method II is normalized by the cost associated with method I, with both methods maintaining a relative error of about 10^{-6}.

Figure 2 first shows a contour plot of the percent error of method II as a function of ρ and θ. This result clearly shows that method II (using five sample points per quarter-cycle in the integration) is accurate, with a relative error on the order of 10^{-6} (a percent error on the order of 10^{-4}), for both moderate and large (near $90°$) values of θ.

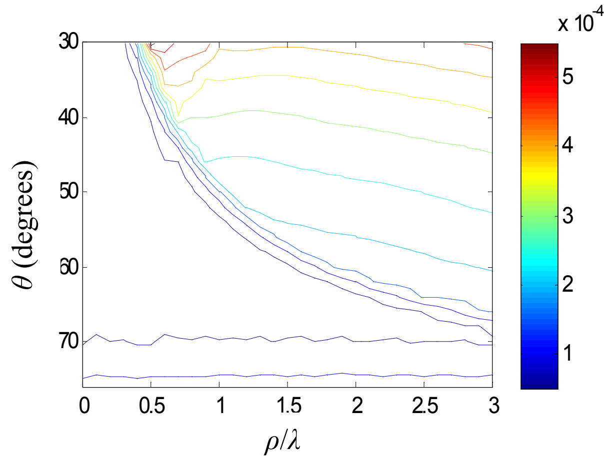

Figure 2. A contour plot of the percent error in method II.

Figure 3 then shows a contour plot of the normalized cost of method II relative to method I. In method I, enough terms were taken in the series (5) to ensure a relative error of about 10^{-6}, while method II employs a fixed (five) number of sample points per quarter-cycle in the integration. On the circled curve where Ratio = 1, both methods have the same cost. Method I is thus more efficient than method II roughly for $\theta < 60^{\circ}$. For smaller values of θ, method I is much more efficient than method II, as expected.

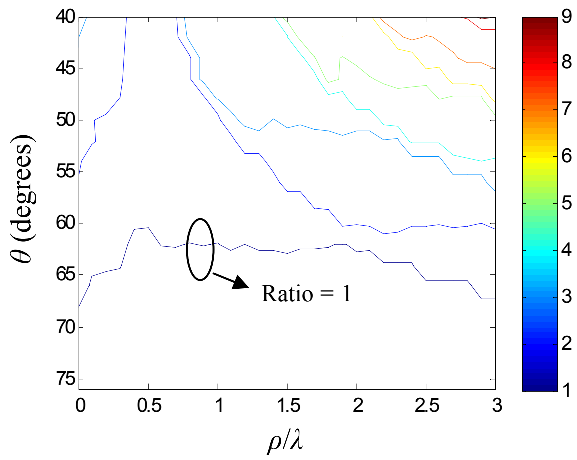

Figure 3. A contour plot of the computational cost of method II normalized by the computational cost of method I.

In method III, four terms in the series (12) were kept (using coefficients B_1 through B_4). Hence, this method was used only in a region of the (ρ, z) plane where these four terms were sufficient to provide a relative error less than 10^{-6}. Figure 4 shows a contour plot of the relative error of method III plotted versus ρ and θ. In order to ensure a relative error less than about 10^{-6}, the observation point should remain in the region of the (ρ, z) plane below the bottom curve shown in Fig. 4 (for which the relative error is approximately 10^{-6}). Detailed calculations have shown that computations using method III are always at least five times faster than those using method II over the entire (ρ, z) plane. Hence, the applicability of method III is limited only by its accuracy, restricting its use to the region below the bottom curve in Fig. 4, where the relative error is less than 10^{-6}. Methods I or II must be used above this region for sufficient accuracy.

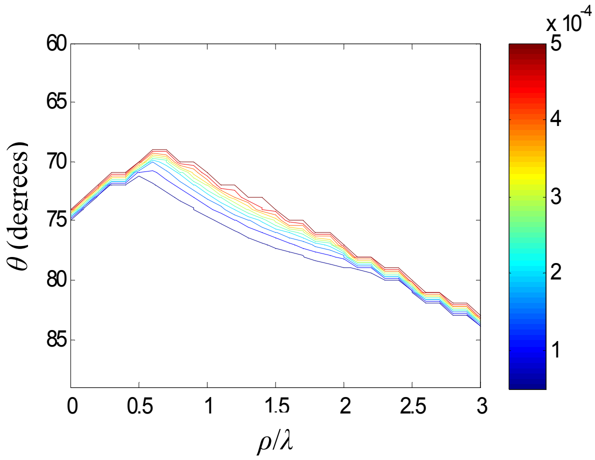

Figure 4. A contour plot of the percent error of method III.

Figure 5 summarizes the regions where each method should be used to ensure maximum overall efficiency. The Ratio = 1 curve of Fig. 2 is the blue (solid) curve in Fig. 5; the red (dashed) curve in Fig. 5 is the same as the lowest curve in Fig. 4. (i.e., the boundary below which method III has a relative error of less than 10^{-6}). The region where each method is most efficient for the given accuracy criterion is indicated in the figure.

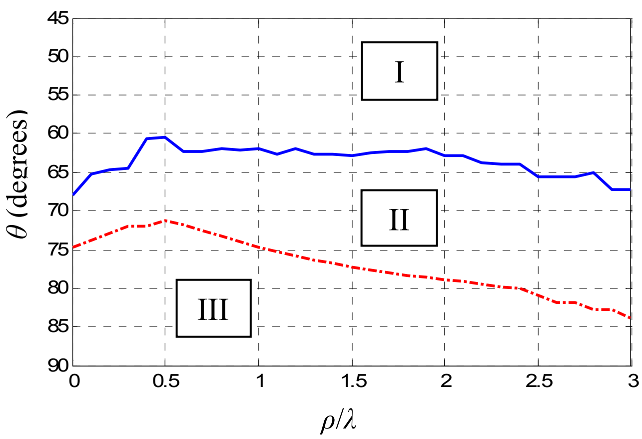

Figure 5. Three different regions spanning the (ρ, z) plane. In each of the three labeled regions, the method indicated is the most efficient.

IV. Conclusions

Evaluation of the potential G_z from a half-line source becomes a major computational cost in using acceleration and/or interpolation techniques for evaluating Green's functions in multilayer media. Hence, efficient methods for calculating G_z are extremely important. Three different methods were explored and compared in terms of their accuracy and computational cost. The regions in space were determined for which each method is the most efficient when requiring a relative error of 10^{-6}. As expected, for relatively small values of θ, method I is most efficient, whereas for values of θ near 90°, method III is the most efficient. Method II is the most efficient in an intermediate region.

References

[1] K. A. Michalski and D. Zheng, "Electromagnetic scattering by sources of arbitrary shape in layered media, Part I: Theory," *IEEE Trans. Antennas Propag.*, vol. 38, no. 3, pp.335-344, Mar. 1990.

[2] M. Abramowitz and I. A. Stegun, *Handbook of Mathematical Functions*, 10th ed., pp. 227–253, Washington, D.C., 1972.

[3] D. R. Wilton, *Computational Methods*, Ch. 1.5.5 in *Scattering: Scattering and Inverse Scattering in Pure and Applied Science*, R. Pike and P. Sabatier, Eds., UK: Academic Press, 2002.

[4] G. Valerio, P. Baccarelli, S. Paulotto, F. Frezza, and A. Galli, "Regularization of mixed potential layered-media Green's functions for efficient interpolation procedures in planar periodic structures," *IEEE Trans. Antennas Propag.*, vol. 57, no. 1, pp. 122-134, Jan. 2009.

[5] P. P. Ewald, "Die berechnung optischer und electrostatischer gitterpotentiale," *Annalen Der Physik*, vol. 64, p. 253–287, 1921.

[6] F. T. Celepcikay, F. Capolino, D. R. Jackson and D. R. Wilton, "Choosing splitting parameters and summation limits in the numerical evaluation of 1-D and 2-D periodic Green's functions using the Ewald method", *Radio Sci.*, vol. 43, 2008, RS6S01, doi:10.1029/2007RS003820.

[7] W. A. Johnson, L. I. Basilio, J. D. Kotulski, R. E. Jorgenson, L. K. Warne, R. S. Coats, D. R. Wilton, N. J. Champagne, F. Capolino, J. Brian Grant, and M. A. Khayat, "EIGER™: An open-source frequency-domain electromagnetics code," *IEEE Intl. Symp. Antennas Propag.*, Honolulu, Hawaii, USA, 10-15 June 2007.